Thermal Assembly of Polysilicon Microstructures

Gary K. Fedder and Roger T. Howe

University of California at Berkeley
Department of Electrical Engineering and Computer Sciences
and the Electronics Research Laboratory
Berkeley Sensor & Actuator Center
Berkeley, California 94720 USA

ABSTRACT

Thermal microassembly techniques are demonstrated which extend the capabilities of surface micromachining technology. Bridges are cleanly severed by application of a single 30 mA, 100 μs pulse. Delicately suspended microstructures are supported by tee bridges during wet etching of phosphosilicate glass, in order to reduce yield loss due to breakage and stiction to the substrate during rinsing and drying. The supports are subsequently severed to release the structure. Mechanical contacts are welded together with 30 mA of current, with a microprobe used to force together the contacts. Qualitative destructive tests indicate that the welded contact is robust. Electrostatic force applied by interdigitated electrodes is insufficient to initiate welding of polysilicon, possibly because the native oxide film must be penetrated to allow current to pass through the contact. Current vs. voltage measurements of polysilicon microbridges agree well with a first-order model, in which heat conduction and convection in air are neglected. Values of the voltage needed to melt the bridge are found to vary with bridge dimensions, because the bridge anchors are not perfect heat sinks.

I. INTRODUCTION

A key feature of surface micromachining is that micromechanical systems, consisting of flexures, linkages, and bearings can be fabricated *in situ* on the silicon substrate, thereby eliminating painstaking and costly microassembly steps [1]. Since these structures are fabricated from deposited thin films, residual strain in the structural layer is an important design constraint. For the case of polysilicon films, considerable work has been done over the last several years to control residual strain for specific applications [2, 3, 4]. It is not possible, however, to have functional microstructures with arbitrarily large lateral dimensions. For example, clamped-clamped microbridges, which are useful for resonant strain gauges [5, 6, 7] require extremely tight control of the average residual strain and also its variation through the film thickness in order to achieve reproducible resonant frequencies. In the case of heavily phosphorus-doped (coarse grain) polysilicon films (which are useful for electrostatically driven and sensed microbridges), such precise control of residual strain has not been achieved to date. For specific applications, it may be possible to select flexure designs which allow release of the average residual strain [8].

Given the limitations of thin films as mechanical materials, how can surface micromachining be modified or extended to fabricate microstructures which are free of residual stress? One avenue is to implement some form of post-fabrication trimming procedure. In this paper, we investigate resistive heating to separate, weld, or deform polysilicon microstructures, subsequent to release from the substrate. The techniques are based on the ability to heat polysilicon microstructures to high temperatures with little power [9, 10, 11]. As we will describe, these thermal microassembly procedures are accomplished under electrical control, without the need for micromanipulation. Additional motivations for post-micromachining assembly are the control or elimination of clearances in microbearings, pre-stressing springs, and active alignment of critical elements. In a companion paper [12], pre-biased lateral flexures are described which also have application to post-micromachining adjustment and assembly. Self-adjusting microstructures and thermal microassembly are both aimed at enhancing the capabilities of surface micromachining technology by means of adjustments and modification to the microstructure after its release from the substrate.

After outlining the fabrication process for the polysilicon test structures, we develop a first-order model for the resistive heating of polysilicon microbridges up to the melting point. Resistive welding and cutting on the macro scale provides some qualitative insight into these processes with polysilicon microbridges. Resistive heating can raise the temperature of polysilicon bridges above the boiling point while dissipating less than 100 mW of power. Experimental measurements of I-V characteristics for polysilicon microbridges are presented, which are in general agreement with the first-order model. We describe one application of thermal microassembly: the severing of temporary support beams which stabilize a large, delicately suspended microstructure during etching of the sacrificial phosphosilicate glass (PSG) layer. A released microstructure can also be deflected laterally by electrostatic forces and welded to anchors by local resistive heating. Finally, we assess the research problems which need attention in order to develop further thermal microassembly.

II. FABRICATION

Several polysilicon bridges and welding structures have been fabricated using two similar processes. A schematic drawing of a completed bridge is shown in Figure 1 for the first process. In both processes, silicon nitride is deposited over thermal silicon dioxide to electrically isolate structures from the silicon substrate. The first process includes a 3000 Å *in situ* doped polysilicon interconnect layer. A layer of 2 μm-thick PSG is deposited as a sacrificial spacer for the polysilicon

CH2957-9/91/0000-0063$01.00 © 1991 IEEE

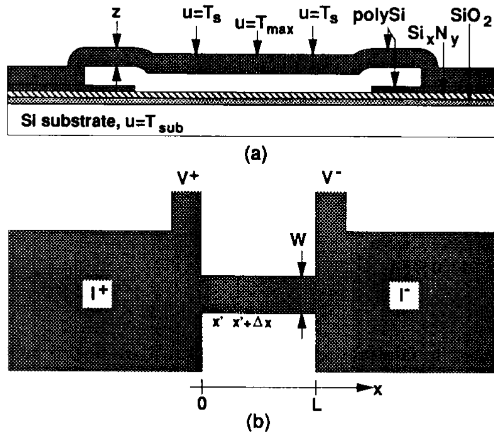

Figure 1. Schematic drawing of a polysilicon microbridge used for I-V measurements. (a) Side view. (b) Top view. Current is applied from I^+ to I^-. Voltage is sensed between V^+ and V^-.

microstructures. Dimples are fabricated on the underside of the final polysilicon structure by patterning 3 μm × 3 μm openings over the sacrificial PSG and doing a timed wet etch in 5:1 BHF. An undoped, 2 μm-thick film of LPCVD polysilicon is deposited at 605 °C, 250 sccm SiH_4, and 550 mTorr, producing a slightly tensile film. This deposition pressure is higher than the 320 mTorr used for very low strain films at 605 °C in previous work on undoped polysilicon deposited on PSG [13]. Results for undoped films deposited on thermal oxide are consistent with a tensile film [14]. After deposition, an additional 0.5 μm of PSG is deposited. A one-hour, 950 °C anneal degenerately dopes the polysilicon and eliminates stress gradients in the film. The structures are defined by CCl_4 plasma etching and released in 10:1 HF. One process includes a CHF_3/CF_4 plasma etch of the sacrificial PSG prior to polysilicon deposition to allow for anchoring of the structures to the substrate. The second process uses a timed wet etch of the PSG sacrificial layer in order to leave oxide mesas for support of the structures.

III. THEORY

Little previous work could be found about modeling of polysilicon microbridges at temperatures up to the melting point. The analysis of polysilicon fuses in ICs is a different problem, since conduction to the substrate under the resistor dominates the heat transfer [15]. A one-dimensional model, including heat conduction and convection through air, has been used to explain thermal characteristics of polysilicon microbridges [11]. For sufficiently short bridges in air, heat is conducted primarily out the ends of the bridge to the supporting structure. Conduction and convection through the ambient atmosphere and radiative terms can be neglected. The temperature distribution in the bridge can be approximated as one-dimensional, varying lengthwise.

The heat flow equation is derived by examining a differential element of the bridge of width w, thickness z, and length Δx (Figure 1b). Under steady-state conditions, ohmic power generated in the element is equal to heat conduction out of the element.

$$\kappa_p A \left(\left.\frac{\partial u}{\partial x}\right|_x - \left.\frac{\partial u}{\partial x}\right|_{x+\Delta x} \right) = J^2 \rho_o (1 + \xi (u - T_o)) A \Delta x \quad (1)$$

where $A = wz$ is the cross-sectional area of the bridge, κ_p is the thermal conductivity of polysilicon, $u(x)$ is the temperature of the bridge, J is the current density, and $\rho(u)$ is the electrical resistivity of the bridge. The resistivity is assumed to have a linear temperature coefficient, ξ, such that $\rho(T_o) = \rho_o$.

$$\rho = \rho_o (1 + \xi (u - T_o)) \quad (2)$$

Combining Equations (1) and (2) and taking the limit as $\Delta x \rightarrow 0$ produces the following second-order differential equation.

$$\kappa_p \frac{\partial^2 u}{\partial x^2} = -J^2 \rho_o (1 + \xi (u - T_o)) \quad (3)$$

Solving Equation (3) and using the boundary conditions, $u|_{x=0} = u|_{x=L} = T_s$ gives the temperature along the length of the bridge.

$$u(x) = \left(T_s - T_o + \frac{1}{\xi} \right) \frac{\cos \gamma (2x/L - 1)}{\cos \gamma} + T_o - \frac{1}{\xi} \quad (4)$$

where $\gamma \triangleq JL\sqrt{\rho_o \xi}/2$.

The maximum temperature, $T_{\max}$, is found at the center of the bridge.

$$T_{\max} = \frac{T_s - T_o + \frac{1}{\xi}}{\cos \gamma} + T_o - \frac{1}{\xi} \quad (5)$$

The total resistance of the bridge is found by integrating the differential resistance, $(\rho/A)dx$ across the bridge.

$$R = \frac{\rho_o L}{A} (1 + \xi (T_s - T_o)) \frac{\tan \gamma}{\gamma} + R_s \quad (6)$$

R_s is a constant series resistance term, which is present because the voltage sense leads (V^+ and V^- in Figure 1b) do not physically contact the bridge at $x = 0$ and $x = L$. Placing sense leads at the end of the bridge would have altered the temperature distribution of the bridge.

The voltage across the bridge is simply the ohmic drop, $V = IR$.

$$V = \frac{I \rho_o L}{A} (1 + \xi (T_s - T_o)) \frac{\tan \gamma}{\gamma} + IR_s \quad (7)$$

It is interesting to note that voltage as a function of maximum temperature can also be found by an alternative derivation [16] if R_s is neglected.

$$V = \sqrt{8 \kappa_p \rho_o \left((1 - \xi T_o)(T_{\max} - T_s) + \frac{\xi}{2} (T_{\max}^2 - T_s^2) \right)} \quad (8)$$

Since the anchor pads are not perfect conductors of heat, the temperature at the ends of the bridge, T_s, will not be constant; T_s varies with bridge geometry and power dissipation. Heat conducted through the pad can be modeled as a linear relationship, $\alpha(T_s - T_{\text{sub}})$, where α is the effective thermal conductance of the pad (with units of W/°C) and T_{sub} is the substrate temperature. In steady-state, total heat flow out the ends of the bridge must equal heat flow through the pads, giving an equation for T_s.

$$T_s = \frac{\alpha T_{\text{sub}}/A + J\sqrt{\rho_o \kappa_p / \xi}\,(1 - \xi T_o) \tan \gamma}{\alpha/A - J\sqrt{\rho_o \kappa_p \xi}} \quad (9)$$

An experimental value for thermal conductivity of degenerately doped polysilicon has been found to be 32 W-m/°K [10]. Temperature variation in single-crystal silicon thermal conductivity [17] suggests that polysilicon will have a significant temperature dependence at high temperatures.

The resistivity of degenerately doped n-type polysilicon exhibits a positive temperature coefficient at temperatures below 300 °C [11, 18]. The potential barrier at the grain boundaries is reduced in heavily doped polysilicon, producing behavior in resistivity similar to single-crystal silicon [19, 20]. At very high temperatures, the temperature dependence of silicon resistivity is not well understood. Below 600 °C, positive values of temperature coefficient for heavily doped silicon resistivity have been measured [21], and negative values of temperature coefficient have been reported above 400 °C [22]. Localized melting of grain boundary layers has been suggested as a mechanism for a decrease in resistivity at sufficiently high temperatures [23].

IV. EXPERIMENTAL RESULTS

Current vs. voltage measurements of several polysilicon microbridges are compared with theoretical values calculated from Equation (7). Experiments with resistive cutting and welding structures are then discussed.

A. I-V Measurements

Current vs. voltage characteristics in air are shown for several values of bridge length (Figure 2a) and bridge width (Figure 2b). As applied voltage is increased, the differential resistance monotonically increases, because of the positive temperature coefficient of resistivity. At a sufficiently high voltage, however, the current through the bridge rises dramatically and eventually open-circuits. Figure 3 shows the resulting melted bridge. The bridge visibly starts to melt when the large increase in current begins to occur. Presumably the melting decreases the resistance, either from deformation or a decrease in resistivity [22, 23]. Larger open-circuit voltages are observed for long, narrow bridges.

Good general agreement is observed between the theoretical curves and the measured data. A measured value for the temperature coefficient at low temperatures, (ξ = 8.3 $\times$ 10^{-4} °C^{-1}) is used in Equation (7) to generate these curves. Values for resistivity, measured for each die, were nominally 3.7 $\times$ 10^{-5} Ω−m. In Figures 2a and 2b, the theoretical curves end when the middle of the bridge reaches the melting point (1412 °C), which will be interpreted as the point when the bridge open-circuits. The finite thermal conductance of the pads accounts for the observed dependence of the open-circuit voltage on bridge geometry. The model does not match measured data for the 20 μm $\times$ 20 μm bridge, possibly because the pad conduction model may break down for very wide bridges. Resistance of polysilicon microbridges has been shown to change with time when operated at high constant temperature [24]. These effects were not included in the present analysis and may account for some of the differences between the model and data at higher temperatures.

Assuming the theoretical model is adequate, bridge temperature during application of the open-circuit voltage can be predicted for various bridge geometries. In particular, long bridges have relatively low temperatures at the ends of the bridge, while short bridges have very high temperatures throughout the bridge. For example, when the temperature

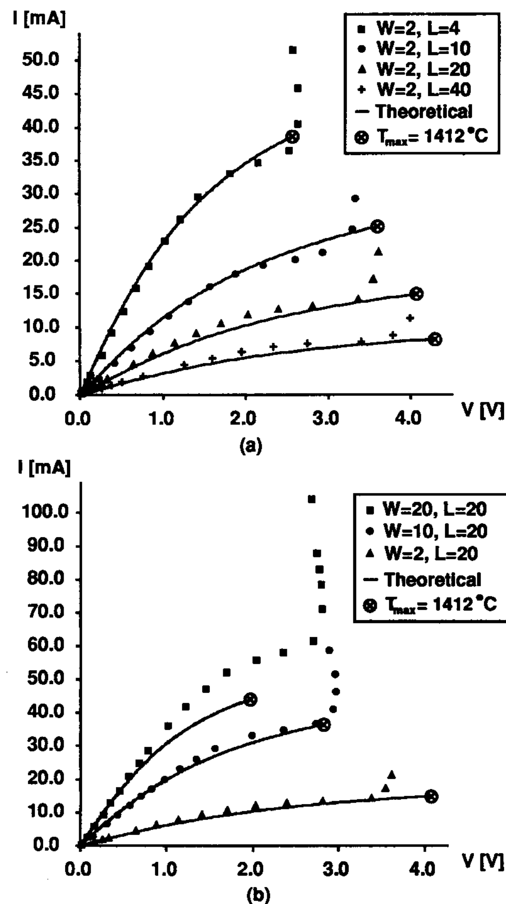

Figure 2. I-V characteristics of several microbridges. (a) Different values of length. (b) Different values of width.

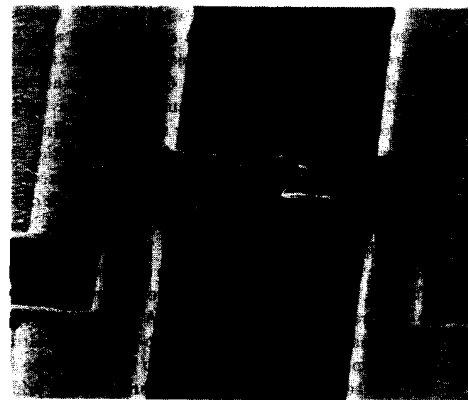

Figure 3. SEM micrograph of an open-circuited 10 μm-wide, 20 μm-long bridge.

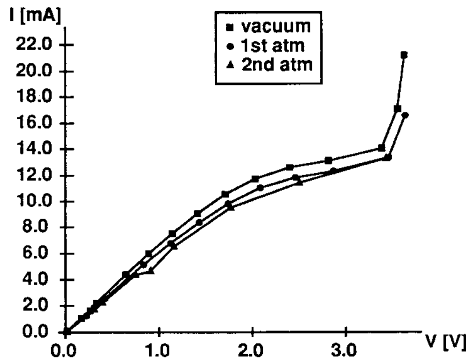

Figure 4. I-V characteristics of 2 μm-wide, 20 μm-long bridges on adjacent dice, showing insensitivity to ambient conditions.

at the center of the bridge is 1412 °C, T_s = 265 °C for a 2 μm-wide by 40 μm-long bridge, while T_s = 1137 °C for a 2 μm-wide by 4 μm-long bridge. Clearly, the temperature of the entire pad cannot be assumed to be at a constant, low value.

Figure 4 shows the I-V curves for three 20 μm-long bridges on three adjacent dice of the same wafer. Two of the bridges were measured in air, while the third bridge was measured in a vacuum probe station pumped down to 3 $\times$ 10^{-4} Torr. Each of the three bridges has a slightly different resistance value, due to process parameter variations across the wafer. Since the values of the open-circuit voltage of each bridge are nearly the same, effects of heat conduction and convection through air are shown to be small. In Figure 4, no large increase in current is noticeable prior to the open-circuit for the bridge in vacuum; however, some increases are seen with other bridges tested in a vacuum.

B. Resistive Cutting

Resistive cutting allows the electrical removal of temporary micromechanical supports. Temporary supports could hold delicate microstructures in place during a wet etch of sacrificial PSG, and away from the substrate while drying. One microstructure designed for this application, a "tee" bridge, is shown in Figure 5a. Current flows through the supporting bridge, which boils the polysilicon and frees the attached beam. Figure 5b shows the severed tee bridge after application of a single 100 μs, 300 mA pulse. Current does not pass through the 2 μm-wide suspension beam, thereby leaving the released microstructure undamaged by resistive heating. No residual material is deposited on the substrate from the cutting operation. The polysilicon bridge had probably exceeded the boiling point, thereby vaporizing the bridge. A view of the entire microstructure (Figure 5c) shows the cantilever beam which was created by resistive cutting.

Although voltages from 3–5 V are sufficient to open-circuit a bridge, much larger voltages are needed to form a wider gap and reliably sever a bridge. A current source is preferred for resistively cutting bridges, so that ohmic drops across contacts, pads, and interconnect do not affect the input power. In a series connected array of bridges, one bridge will open-circuit first, removing the power source from the circuit. Therefore, only one cut can be made at a time. Voltage sources can produce many cuts in parallel, but it is harder to

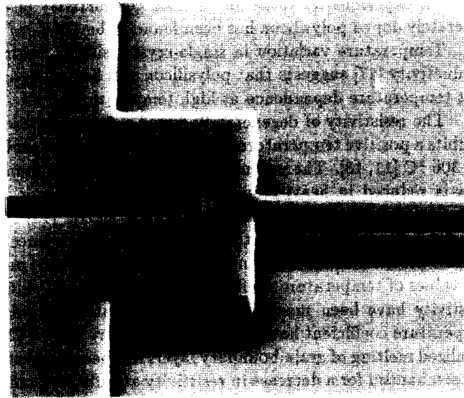

(a)

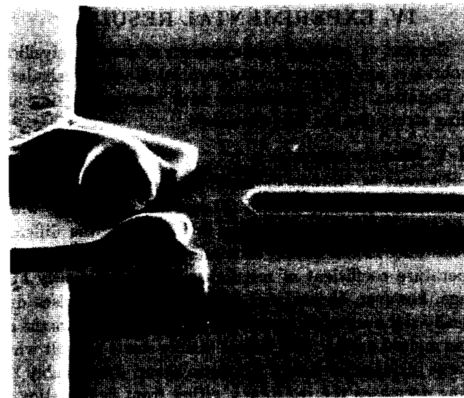

(b)

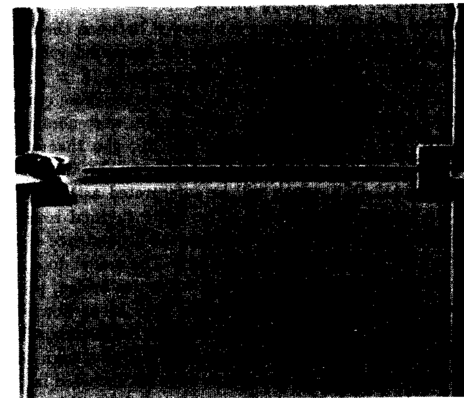

(c)

Figure 5. SEM micrograph of a polysilicon tee bridge. (a) Before resistive cutting. (b) After resistive cutting. (c) View of released cantilever beam.

control the input power and produce clean cuts. These fusible microbridges could be used as the basis for an alternative to conventional polysilicon fuses in electrical trimming.

C. Resistive Welding

Structures to be used for resistance welding must provide maximum temperature at the mechanical joint, otherwise the structure will be destroyed prior to creating a welded joint. In particular, designs should be avoided which pass welding current through mechanical flexures. A first-generation welding test structure is shown in Figure 6. The current path is symmetric, beginning at one anchored pad (on the right side in Figure 6), through a cantilevered support which contacts a large structural plate, and then back through a second contact to the other pad. A plunger, shown on the left side of Figure 6, allows a probe tip to close the 2 μm gap separating the contacts and to supply sufficient force for welding. The two cantilever supports are 40 μm-wide by 60 μm-long, with four pointed teeth at the end of the beams. Several other designs, with different cantilever support dimensions and number and type of teeth, were fabricated.

Delicate microstructures can be attached to the structural plate without being subjected to high temperatures. Unlike short microbridges, conduction through air under the plate is significant. Much of the plate experiences a low current density, allowing the outer regions of the plate to sink heat from hotter areas. The cantilever supports extend the contact away from the pad, which would otherwise act to reduce temperature at the contact. Contact width should be small relative to the support width, both to increase power generation near the contact and to avoid melting of the supports. Contact area should be maximized, to provide current flow across the junction with a minimal amount of applied force.

Figure 7a shows a completed welding structure after 30 mA of current was applied for several minutes in air. The resulting structure is bonded to the anchored supports. A close-up view of the lower joint (Figure 7b) shows a clean weld, but an out-of-plane alignment. A large force is required to create an electrical connection through the joint, making perfect alignment impossible. A thin layer of native oxide, covering the polysilicon contacts, acts as a barrier to conduction. Even with the highly anisotropic plasma etch, the polysilicon sidewalls have a slight slope, which reduces the contact area. We believe that the large applied force is necessary to penetrate this oxide layer. Electrostatic forces produced by micromechanical actuators are not nearly large enough to reliably initiate the polysilicon welding process.

Both flexures supporting the structural plate were broken by a probe tip without affecting the welded joints. A probe tip was then used to break the welded joints by pushing on the plate. The upper joint in Figure 7a did not fail. Instead, a large section of the structural plate was broken. The lower joint was marginal, since a break occurred near the weld. The applied current was raised slightly higher on other samples, resulting in uncontrollable deformation of the structure until the connection open-circuited.

The absence of oxygen may improve the weld quality, since no thermal oxidation of the polysilicon can take place. However, when operating in a vacuum, the entire structure be-

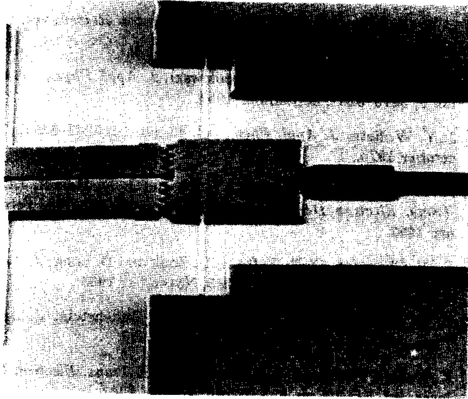

Figure 6. SEM micrograph of a first-generation welding test structure. The structural plate in the center is to be welded to the 40 μm-wide, 60 μm-long cantilever supports, located on the left. A plunger for applying force with a probe tip is located on the right.

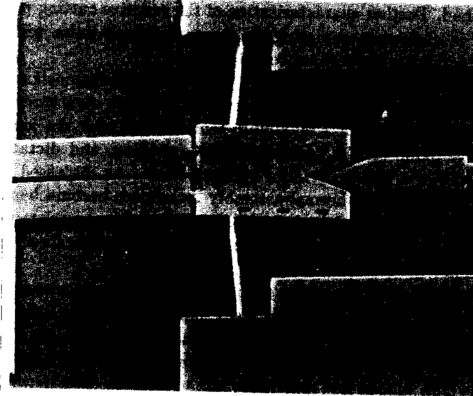

(a)

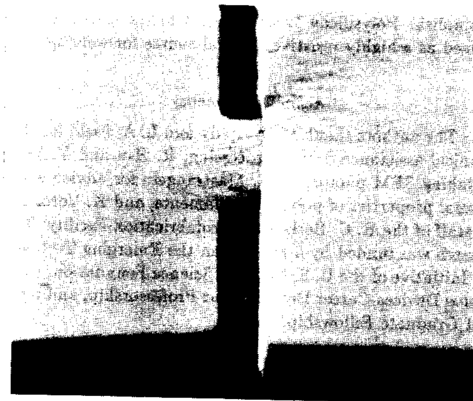

(b)

Figure 7. SEM micrograph of a completed weld. (a) View of the entire structure. (b) Close-up of the lower joint showing a clean weld and out-of-plane alignment.

comes unacceptably hot, making welding impossible without first destroying the structure. Preliminary experiments have shown that the location of maximum temperature can be adjusted by changing pressure in the vacuum chamber. Nitrogen was used to raise the pressure. An inert gas, such as argon, may be better suited for such experiments, since a thin film of silicon nitride can form on polysilicon in a nitrogen ambient at elevated temperatures.

V. CONCLUSIONS

A first-order model has been developed which predicts the general behavior of polysilicon microbridges up to the melting point. Conduction through the ends of the bridge is the only significant heat transfer mechanism. The finite thermal conduction of the anchor pads produces an open-circuit voltage which varies between 2–5 V, varying with bridge geometry. Prior to the open-circuit voltage, the bridge resistance drops dramatically, perhaps because of deformation.

Resistive cutting of polysilicon microbridges has been demonstrated using 300 mA current pulses. Suspended microstructures can be released, undamaged, by using this method. Further characterization of the resistive cutting process is underway, exploring the lower limits on pulse width and total energy required to cut bridges.

An initial polysilicon weld joint has been demonstrated with limited success. Proper design of welding structures is necessary to ensure a maximum temperature near the joint. Native oxide on the contacts inhibits welding, and dictates the use of a relatively large bonding force. As discussed in the introduction, thermal assembly techniques become beneficial when micromanipulation is eliminated. More work must be done to see if resistive welding with electrostatic forces is feasible.

Depositing aluminum near the contacts may prove useful in making better polysilicon weld joints and will be investigated. Related work has involved formation of aluminum filaments in polysilicon bridges by diffusion of metal from contact pads [25]. Silicon and aluminum mix to form an eutectic with a minimum melting point of 577 °C. By forming the eutectic near the mechanical contacts, welding may become easier to accomplish. Polysilicon areas adjacent to the contacts could be used as a highly resistive thermal source for welding.

Acknowledgements

The authors thank M. W. Judy and L. A. Field for their technical assistance during processing, R. Hsu and V. Wong for taking SEM photos, C. H. Mastrangelo for advice about thermal properties of polysilicon filaments, and K. Voros and the staff of the U. C. Berkeley Microfabrication Facility. This research was funded by a grant from the Emerging Technologies Initiative of the U. S. National Science Foundation, by an Analog Devices Career Development Professorship, and by an IBM Graduate Fellowship.

REFERENCES

[1] R. T. Howe, J. Vac. Science and Tech., part B, vol. B6, 1809–1813, 1988.

[2] R. T. Howe and R. S. Muller, *Sensors and Actuators*, vol. 4, 447–454, 1983.

[3] H. Guckel, D. W. Burns, C. R. Rutigliano, D. K. Showers and J. Uglow, *Technical Digest*, 4th Inter. Conf. on Solid-State Sensors and Actuators, Tokyo, Japan, 277–282, June 1987.

[4] H. Guckel, J. J. Sniegowski, T. R. Christenson, and F. Raissi, *Sensors and Actuators*, vol. A21-A23, 346–351, February 1990.

[5] R. T. Howe, *Technical Digest*, 4th Inter. Conf. on Solid-State Sensors and Actuators, Tokyo, Japan, 843–848, June 1987.

[6] J. J. Sniegowski, H. Guckel, and T. R. Christenson, *Technical Digest*, IEEE Solid-State Sensor and Actuator Workshop, Hilton Head Island, South Carolina, 9–12, June 1990.

[7] C. Linder and N. F. de Rooij, *Sensors and Actuators*, vol. A21-A23, 1053–1059, April 1990.

[8] W. C. Tang, T.-C. H. Nguyen and R. T. Howe, *Proceedings*, IEEE Micro Electro Mechanical Systems Workshop, Salt Lake City, Utah, February, 1989.

[9] H. Guckel and D. W. Burns, *Technical Digest*, 3rd Inter. Conf. on Solid-State Sensors and Actuators, Philadelphia, Penn., 364–366, June 1985.

[10] Y. C. Tai, C. H. Mastrangelo and R. S. Muller, *J. Appl. Phys.*, vol. 63, no. 5, 1442–1447, March 1988.

[11] C. H. Mastrangelo, M.S. Thesis, Dept. of Electrical Engineering and Computer Sciences, University of California at Berkeley, Chapter 2, May 1988.

[12] M. W. Judy, R. T. Howe, Y.-H. Cho, and A. P. Pisano, *Proceedings*, IEEE Micro Electro Mechanical Systems Workshop, Nara, Japan, January–February 1991.

[13] L. S. Fan and R. S. Muller, *Technical Digest*, IEEE Solid-State Sensor and Actuator Workshop, Hilton Head Island, South Carolina, 55–59, June 1988.

[14] P. Krulevitch, T. D. Nguyen, G. C. Johnson, R. T. Howe, H. R. Wenk, and R. Gronsky, *Proceedings*, Materials Research Society Fall Meeting, vol. 202, 1990.

[15] D. W. Greve, *IEEE Trans. Electron Devices*, vol. ED-29, no. 4, 719–807, April 1982.

[16] F. Llewellyn Jones, *The Physics of Electrical Contacts*, Clarendon Press, Oxford, 1957.

[17] C. J. Glassbrenner and G. A. Slack, *Physical Review*, vol. 134, no. 4A, 1058–1069, May 1964.

[18] R. E. Jones, Jr. and S. P. Wesolowski, *J. Appl. Phys.*, vol. 56, no. 6, 3278–3281, September 1984.

[19] J. Y. W. Seto, *J. Appl. Phys.*, vol. 46, no. 12, 5247–5254, December 1975.

[20] N. C.-C. Lu, L. Gerzberg, C.-Y. Lu and J. D. Meindl, *IEEE Trans. Electron Devices*, vol. ED-30, no. 2, 137–149, February 1983.

[21] P. W. Chapman, O. N. Tufte, J. D. Zook and D. Long, *J. Appl. Phys.*, vol. 34, no. 11, 3291–3295, November 1963.

[22] D. H. Pontius, W. B. Smith and P. P. Budenstein, *J. Appl. Phys.*, vol. 44, no. 1, 331–340, January 1973.

[23] K. Kato, T. Ono and Y. Amemiya, *IEEE Trans. Electron Devices*, vol. ED-29, no. 8, 137–149, August 1982.

[24] C. H. Mastrangelo, H.-J. Yeh and R. S. Muller, *IEEE Trans. Electron Devices*, to be published, 1991.

[25] D. W. Greve, *J. Appl. Phys.*, vol. 54, no. 6, 3278–3281, June 1983.